Journal of Cell Science 109, 2833-2842 (1996)
Printed in Great Britain © The Company of Biologists Limited 1996
JCS4221

Calcium-dependent bidirectional power stroke of the dynein arms in sea urchin sperm axonemes

Sumio Ishijima[1,*], Miyoko Kubo-Irie[2], Hideo Mohri[2,†] and Yukihisa Hamaguchi[1]

[1]Biological Laboratory, Faculty of Bioscience and Biotechnology, Tokyo Institute of Technology, O-okayama, Meguro-ku, Tokyo 152, Japan
[2]Biological Laboratory, University of the Air, Wakaba, Mihama-ku, Chiba 261, Japan

*Author for correspondence
†Present address: National Institute for Basic Biology, 38 Nishigonaka, Myodaijicho, Okazaki 444, Japan

SUMMARY

Active sliding between doublet microtubules of sea urchin sperm axonemes that were demembranated with Triton X-100 in the presence or absence of calcium was induced with ATP and elastase at various concentrations of Ca^{2+} to examine the effects of Ca^{2+} on the direction of the power stroke of the dynein arms. Dark-field light microscopy of microtubule sliding revealed that the sliding from the axonemes demembranated with Triton and millimolar calcium and disintegrated with ATP and elastase showed various patterns of sliding disintegration, including loops of doublet microtubules formed near the head or the basal body. These loops were often thicker than the remaining axonemal bundle. In contrast, only thinner loops were found from the axonemes demembranated with Triton in the absence of calcium and disintegrated with ATP and elastase at high Ca^{2+} concentrations. Electron microscopic examination of the direction of microtubule sliding showed that the doublet microtubules in the axonemes demembranated in the presence of millimolar calcium moved toward the base of the axonemes by the dynein arms on the adjacent doublet microtubule as well as by their own dynein arms. Doublet microtubules in the axonemes demembranated in the absence of calcium moved toward the base of the axonemes only by their own dynein arms. Similar observations have been obtained from the axonemes from which the outer dynein arms were selectively extracted. From these observations, we can conclude that the dynein arms generate force in both directions and this feature of the dynein arms arises from at least the inner dynein arms.

Key words: Dynein arm, Microtubule sliding, Power stroke, Sperm flagellum

INTRODUCTION

It is now well established that the basis for ciliary and flagellar movements is an ATP-dependent sliding between adjacent outer doublet microtubules (Gibbons, 1981), but much remains to be learned about how this active sliding is constrained to give the typical beat patterns of cilia and flagella. On the basis of our observations that the chirality of the bending waves of reactivated sea urchin sperm flagella is changed by the free Ca^{2+} concentration in the solution, we have proposed a model for conversion of active sliding into flagellar bending; bending waves are generated by localized sliding between doublet microtubules, sliding which propagates from the base of the flagellum toward the tip along the axoneme and at the same time spreads about the axoneme in either direction, the order of doublets being 1, 2, 3 etc. or 9, 8, 7 etc. (Ishijima and Hamaguchi, 1993). A simple hypothesis to explain the reversals of the direction of the localized sliding transmitted about the axoneme is that the direction of the power stroke of the dynein arms can change due to Ca^{2+} concentration (Ishijima and Hamaguchi, 1993).

Most experiments determining the polarity of microtubule sliding in the axoneme have demonstrated that the outer doublet microtubules move with a single polarity; the dynein arms produce force from base to tip only (Sale and Satir, 1977; Mogami and Takahashi, 1983; Sale, 1986; Fox and Sale, 1987; Woolley and Brammall, 1987). On the contrary, microtubules bidirectionally slide on the tracks of dynein molecules aligned with the same polarity in the presence of Nonidet P-40 (Mimori and Miki-Noumura, 1994) and the cytoplasmic dynein prepared from the giant amoeba, *Reticulomyxa*, also caused bidirectional movements of latex beads along its microtubules in vitro (Euteneuer et al., 1988). Considerable evidence indicates that calcium ions play an important role in the regulation of ciliary and flagellar beating, but experiments on the effect of calcium ions on microtubule sliding in axonemes are contradictory; calcium ions have no effect on the microtubule sliding (Walter and Satir, 1979; Mogami and Takahashi, 1983); calcium ions are necessary for the microtubule sliding (Tamm, 1989); calcium ions inhibit the gliding movement of doublet microtubules on *Tetrahymena* ciliary dyneins (Mori and Miki-Noumura, 1992).

To investigate the possibility that the direction of the power stroke of the dynein arms is changed by Ca^{2+}, active sliding between doublet microtubules of demembranated sperm axonemes was induced with ATP and elastase at various con-

centrations of Ca^{2+}. Electron microscopy of the active microtubule sliding revealed that dynein arms pushed the adjacent B-tubule toward either the base or tip of the axonemes when the spermatozoa had been demembranated with Triton X-100 in the presence of Ca^{2+} and disintegrated with ATP and elastase. In contrast, the dynein arms always pushed the adjacent B-tubule toward the tip of the axonemes when the spermatozoa had been demembranated with Triton in the absence of Ca^{2+} and disintegrated with ATP and elastase at a high concentration of Ca^{2+}. Similar observations have been obtained in axonemes from which the outer dynein arms had been selectively extracted.

MATERIALS AND METHODS

Sperm preparations

Concentrated spermatozoa of the sea urchin, *Hemicentrotus pulcherrimus*, were obtained by intracoelomic injection of 10 mM acetylcholine dissolved in artificial seawater (Jamarin U, Jamarin Laboratory, Osaka) and placed in a plastic culture dish (35 mm × 10 mm) kept in a refrigerator until use.

Demembranation and reactivation

To remove the sperm plasma membrane with Triton X-100 and millimolar calcium, 5 μl of the concentrated spermatozoa was placed in a well of a 24-well tissue culture plate containing 0.5 ml of extraction solution consisting of 0.15 M KCl, 10 mM Tris buffer, 1 mM DTT, 0.2 mM EGTA, 0.05% (w/v) Triton X-100, 2 mM $MgSO_4$, and 2 mM $CaCl_2$, pH 8.2. The suspension was then stirred gently for approximately 30 seconds, after which time 10 μl of the mixture was transferred to another well containing 1 ml of reactivation solution consisting of 0.25 M potassium acetate, 10 mM Tris buffer, 1 mM DTT, 2 mM EDTA or EGTA, and various concentrations of $MgSO_4$, $CaCl_2$, and ATP, pH 8.2. The concentrations of $MgSO_4$, $CaCl_2$, and ATP were determined by a computer program developed by Dr Terrence L. Scott (Boston Biomedical Research Institute, Boston, MA), which is based on the original algorithms of Goldstein (1979), in order to obtain the desired $MgATP^{2-}$ or Ca^{2+} concentrations without changing the concentrations of other species in the solutions. EGTA was used for the free Ca^{2+} concentrations of 10^{-9} to 10^{-7} M and EDTA for the free Ca^{2+} concentrations of 10^{-7} to 10^{-4} M (Brokaw, 1986; Bers et al., 1994). To remove the sperm plasma membrane with Triton X-100 in the absence of Ca^{2+}, 5 μl of the concentrated spermatozoa was placed in a well of a 24-well tissue culture plate containing 0.5 ml of extraction solution consisting of 0.15 M KCl, 10 mM Tris buffer, 1 mM DTT, 2 mM EGTA, 0.05% (w/v) Triton X-100, and 1 mM $MgSO_4$, pH 8.2. The suspension was then stirred gently for approximately 30 seconds, after which time 10 μl of the mixture was transferred to another well containing 1 ml of reactivation solution consisting of 0.25 M potassium acetate, 10 mM Tris buffer, 1 mM DTT, 0.1 mM EGTA, 2 mM $MgSO_4$, 0.4 mM $CaCl_2$, and 1 mM ATP, pH 8.2.

For demembranation and outer arm extraction, we used the method of Fox and Sale (1987); 0.6 M KCl was used in the place of 0.15 M KCl and 50 μM cAMP was added to the extraction solutions described above. After incubation in the extraction solutions for 90 seconds, the extracted spermatozoa were transferred to the reactivation solutions, the same solutions described above.

Extraction and reactivation solutions were made from stock solutions just before use. All procedures were done at room temperature (19°C).

ATP, elastase-induced microtubule sliding

Sliding of the doublet microtubules was induced as follows. Concentrated sperm suspensions were treated as described above in either 0.15 or 0.6 M KCl extraction solution. After 30 or 90 seconds, 10 μl of the mixture was transferred to a well containing 1 ml of ATP-free reactivation solution. Approximately 50 μl of the sperm suspension obtained was transferred to a glass slide in an approximately 0.25 mm deep trough formed using quadruple layers of transparent mending tape (Scotch Magic Tape No. 810, 3M Corp., St Paul, MN) attached to the slide in two parallel strips; the trough was then covered with a glass coverslip. Microtubule sliding was achieved by applying a small volume of the reactivation solution containing 20 μg/ml elastase (E-0127; Sigma Chemical Co., St Louis, MO) to one end of the chamber while the excess fluid was drained from the opposite end with small pieces of filter paper.

Light microscopy

The course of the microtubule sliding was recorded using a Nikon Optiphot microscope equipped with an oil-immersion dark-field condenser (NA 1.20-1.43), an Olympus ×40 oil-immersion plan apochromatic objective (NA 1.00), and ×10 eyepieces. Images were recorded on VHS 1/2-inch cassette videotape with a Panasonic CCD video camera (WV-BD 400; Matsushita Communication Industrial Co., Ltd, Yokohama), a video timer (VTG-33, For-A Corp., Tokyo), and a Panasonic Super-VHS videocassette recorder (NV-FS900; Matsushita Electric Industrial Co., Ltd, Osaka) in the field mode. Illumination was provided by a Nikon high-pressure mercury arc lamp (HBO-100 W/2). For detailed field-by-field analyses, images recorded on the videotape were traced from a video monitor (TN-96, Panasonic, Osaka) onto transparent plastic sheets using a fine-point marker. The sliding rate was calculated by dividing the length of the extruded microtubules by the total time for sliding. For preparation of the figures, images on the video monitor were photographed with a frozen field using Fuji Neopan F 35 mm film.

The flagellar movement of intact and reactivated spermatozoa swimming close to the coverslip surface was recorded using a Nikon Optiphot microscope equipped with a phase-contrast condenser, a ×40 BM plan achromatic objective, and ×10 eyepieces. Images were recorded on VHS 1/2-inch cassette videotape at 200 frames per second with a high-speed video system (MHS-200; Nac, Inc., Tokyo) (Ishijima, 1995). Beat frequencies of sperm flagella beating at more than approximately 10 Hz were determined by stroboscopic dark-field microscopy; the flash frequency of a strobe (model 100, Chadwick-Helmuth Corp., El Monte, CA) triggered by a stimulator (MSE-3R; Nihon Kohden Kogyo Co., Ltd, Tokyo) was adjusted to the beat frequency of the sperm flagella, and the period of the square wave generated by the stimulator was measured with an oscilloscope (5103N, Sony-Tektronix Co., Tokyo). Beat frequencies of less than 10 Hz were determined from images recorded on videotape using a Super-VHS videocassette recorder by measuring the mean period required for one complete beat.

The circular motion of the reactivated spermatozoa at the upper surface of the sperm suspension was recorded using a Nikon Optiphot microscope fitted with a phase-contrast condenser, a ×20 BM plan achromatic objective, and ×10 eyepieces. Images were recorded using a Super-VHS videocassette recorder, and the direction of the circular motion of the reactivated spermatozoa was determined from these images in the video monitor by playing back the tape recorded for at least 10 seconds (Ishijima and Hamaguchi, 1993).

Electron microscopy

For observation of ATP-induced sliding disintegration of the axonemes, demembranated spermatozoa were placed on carbon-film-coated copper grids. The preparations were rinsed with a drop of reactivation solution lacking ATP and floated on a drop of reactivation solution containing elastase. After 45 seconds, the grids were transferred to a drop of 1% glutaraldehyde in the same reactivation solution, rinsed with deionized water, and stained with several drops of 4% aqueous uranyl acetate. These were then fully drained off and the grids allowed to dry. To determine the direction of microtubule sliding

between any two doublet microtubules, it was necessary to identify the distal and proximal directions along any doublet microtubule as well as distinguishing the A- and B-tubule of each doublet microtubule. The head or the basal body provided the marker for the proximal end of the doublet microtubule (Euteneuer and McIntosh, 1981; Fox and Sale, 1987; Sloboda, 1992), while the A-tubule was distinguished from the B-tubule by the origin of the dynein arms and its greater width.

To verify that the outer dynein arms were completely extracted in the 0.6 M KCl extraction solution containing 2 mM $CaCl_2$, demembranated spermatozoa were fixed by adding an equal volume of reactivation solution containing 2% glutaraldehyde (effecting a final glutaraldehyde concentration of 1%). After 10 minutes, this suspension was centrifuged at 4,000 ***g*** for 10 minutes in a Sakuma MS-1 swinging bucket rotor (Sakuma Seisakusho Co., Ltd, Tokyo). The resultant pellets were fixed in a solution containing 0.5% tannic acid, 0.1 M cacodylate buffer, and 2.5% glutaraldehyde. Samples were postfixed in 1% OsO_4 in cacodylate buffer, dehydrated through a series of ethanol solutions at room temperature, and embedded in Quetol 812. Thin sections were doubly stained with uranyl acetate and lead citrate. Electron micrographs were taken with a JEOL-1200EX II electron microscope operated at 80 kV.

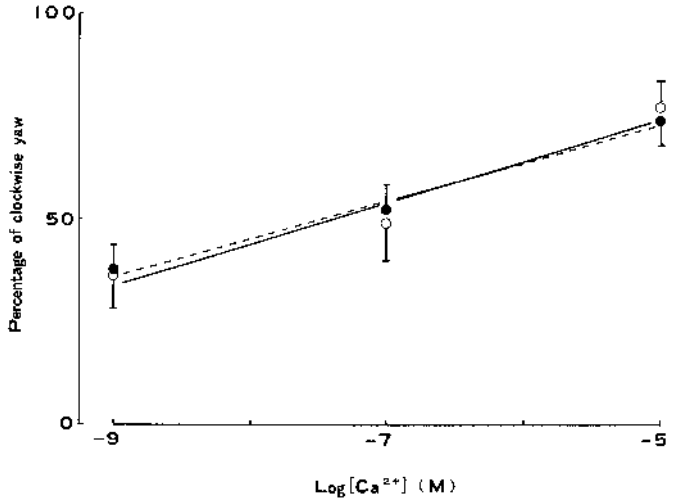

Fig. 1. Effect of Ca^{2+} on the direction of yawing spermatozoa reactivating with 0.5 mM $MgATP^{2-}$. Open circles show mean values obtained from the reactivated spermatozoa with intact dynein arms. Solid circles show mean values from the reactivated spermatozoa without outer dynein arms. Each point is the mean of values obtained from three experiments, with approximately 30 spermatozoa measured in each experiment. Vertical bars represent standard deviations. The lines are obtained by weighted least squares fitting of the equation: the continuous line is for the intact arm spermatozoa and the broken line for the outer arm-depleted spermatozoa.

RESULTS

Active sliding between doublets in sperm axonemes demembranated with Triton X-100 and millimolar calcium

When spermatozoa were demembranated with Triton X-100 in the presence of 2 mM $CaCl_2$ and reactivated with $MgATP^{2-}$, they swam in circular paths near an interface. Parameters of the bending waves of reactivated sperm flagella depended upon the conditions for reactivation: beat frequency increased with the $MgATP^{2-}$ concentration in the reactivation solution (Table 1); waveforms were fairly symmetrical at low calcium concentrations and were asymmetrical at high calcium concentrations (data not shown) as reported earlier (Brokaw, 1991; Ishijima and Hamaguchi, 1993). The direction of the circular motion of reactivated spermatozoa swimming at the upper surface of the sperm suspension depended upon the Ca^{2+} concentration as well; the percentage of the reactivated spermatozoa yawing clockwise gradually increased with the Ca^{2+} concentration (Fig. 1; Ishijima and Hamaguchi, 1993).

Exposure of the spermatozoa demembranated with Triton and millimolar calcium to $MgATP^{2-}$ and elastase caused microtubule sliding disintegration after a certain period of beating of reactivated sperm flagella, during which period they showed important changes in motility resulting from digestion by elastase as reported in detail by Brokaw (1980). We observed various patterns of sliding disintegration (Fig. 2): doublet microtubules extruded from the axoneme formed loops near the head or the basal body, the extruded microtubules that scattered less light under dark-field illumination than the axonemal bundle (Fig. 2A) or scattered more light than the residual doublet microtubules (Fig. 2B and C). Sometimes the most outer doublet microtubules slid and moved toward the tip of the axoneme (Fig. 2D). Fig. 3 shows sequences of the process of two typical patterns of ATP-induced microtubule sliding in elastase-treated demembranated spermatozoa; the extruded microtubules were thicker (Fig. 3A) and thinner (Fig. 3B) than the residual doublet microtubules. In both cases, the doublet microtubules of the larger loops continued sliding, even though they were in contact with only the doublet microtubules of the smaller loops because their distal ends had left the residual doublet microtubules (Fig. 3). This implies that the microtubule

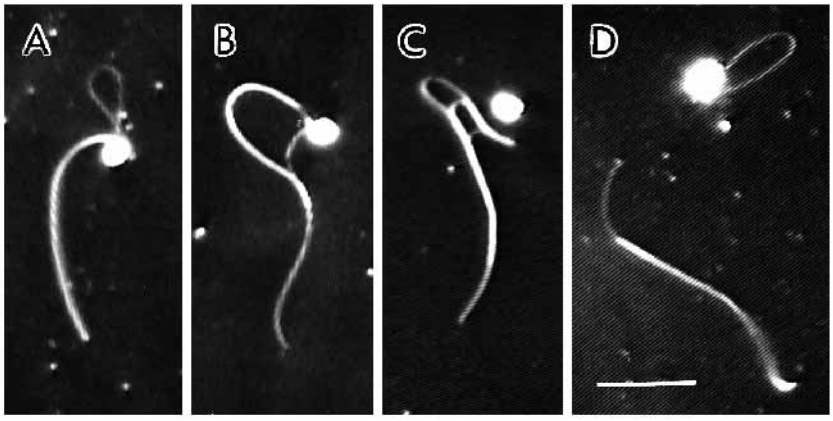

Fig. 2. Dark-field videomicrographs of sliding between doublets of sperm axonemes demembranated with Triton and millimolar calcium and treated with $MgATP^{2-}$ and elastase. Four typical patterns are shown (A-D). Doublet microtubules extruded from the axoneme formed loops near the head or the basal body. The extruded microtubules were not only thinner (A and D) but also thicker (B and C) than the residual doublet microtubules. Bar, 15 μm.

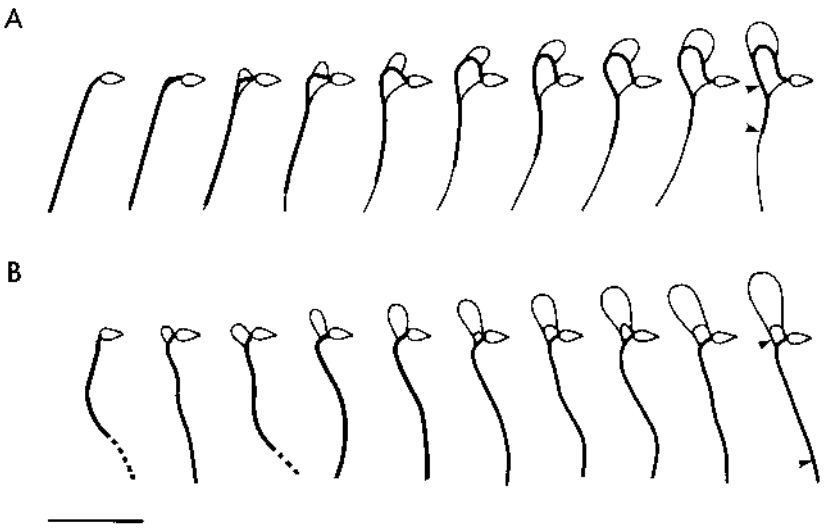

Fig. 3. Tracings from video recordings showing sequences of the process of sliding disintegration in elastase-treated demembranated spermatozoa. The extruded microtubules were thicker (A) and thinner (B) than the residual doublet microtubules. The time interval between successive images was 0.15 second (A) and 0.2 second (B). The out-of-focus segments are drawn as broken lines. The arrowheads define the locations of the distal tips of doublet microtubules sliding out from the bundles of doublet microtubules. Bar, 20 μm.

extrusions were caused by active sliding between the doublet microtubules (see Discussion). Sliding velocity was 14.4±4.1 μm/second (mean ± s.d., n=11) in the reactivation solution containing 0.5 mM $MgATP^{2-}$ and 0.1 μM free Ca^{2+}. To examine the relationship between the direction of the circular motion of reactivated spermatozoa and the pattern of the sliding disintegration, the patterns of ATP-induced sliding disintegration in elastase-treated demembranated spermatozoa that had yaw counterclockwise at the upper surface of the sperm suspension were determined by reconstruction from video recordings. All spermatozoa (22 examples determined) having yaw counterclockwise until disintegration gave the patterns similar to those of Fig. 2B and C, in which the extruded doublet microtubules were thicker than the residual doublet microtubules.

To examine the polarity of microtubule sliding by electron microscopy, we restricted our attention to images where only two or three doublet microtubules were overlapping. Such images showed two patterns: (1) the microtubules of the larger loops slid in the proximal direction relative to the microtubules of the smaller loops by their own dynein arms (45 examples observed) (Fig. 4); to form this pattern of microtubule sliding, the dynein arms have generated a driving force from base to tip; and (2) the microtubules of the larger loops slid in the proximal direction relative to the microtubules of the smaller loops by the dynein arms of the microtubules of smaller loops (72 examples observed) (Fig. 5); the dynein arms have generated force from tip to base.

Table 1. Comparison of beat frequencies of control reactivated spermatozoa with those of outer arm-depleted spermatozoa at several $MgATP^{2-}$ concentrations

$MgATP^{2-}$ (mM)	Control reactivated sperm (Hz)	n*	Reactivated outer arm-depleted sperm (Hz)	n*	Reactivated outer arm-depleted sperm/control reactivated sperm
0.5	31.2±2.5	25	15.3±1.0	16	0.49
0.1	20.0±1.3	25	10.3±0.9	14	0.52
0.02	6.1±0.7	12	4.0±0.8	11	0.66

Values represent mean ± standard deviation. All measurements were carried out at 19°C.

*n, total number of spermatozoa measured in three different experiments.

Active sliding between doublets in calcium-induced quiescent sperm axonemes

When spermatozoa were demembranated with Triton X-100 in the presence of 2 mM EGTA and reactivated with $MgATP^{2-}$ in the presence of high calcium concentration, most spermatozoa became quiescent with their flagella bent into a highly asymmetric cane-like form as reported earlier (Gibbons and Gibbons, 1980; Sale, 1986).

Exposure of the quiescent reactivated spermatozoa to elastase caused the microtubules to disintegrate by sliding (Fig. 6). The patterns of sliding disintegration are comparable to those described by Gibbons and Gibbons (1980) and Sale (1986); doublet microtubules extruded from the

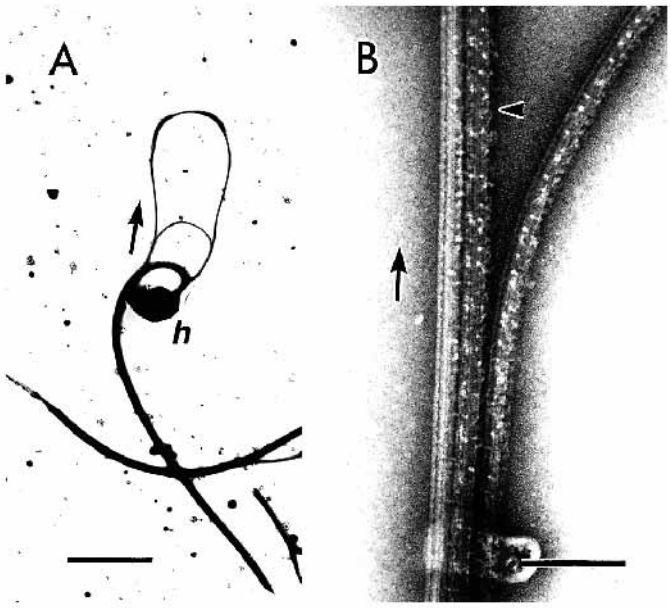

Fig. 4. Electron micrographs of sliding between doublets of sperm axonemes demembranated with Triton and millimolar calcium and treated with $MgATP^{2-}$ and elastase. The head (*h* in A) is a marker of the proximal end of the axonemes. B is a high magnification view of the vicinity of the arrow in A. The dynein arms (arrowhead) generate a driving force from base to tip and cause the doublet to slide proximally (arrow). Bars: 4 μm in A, 0.2 μm in B.

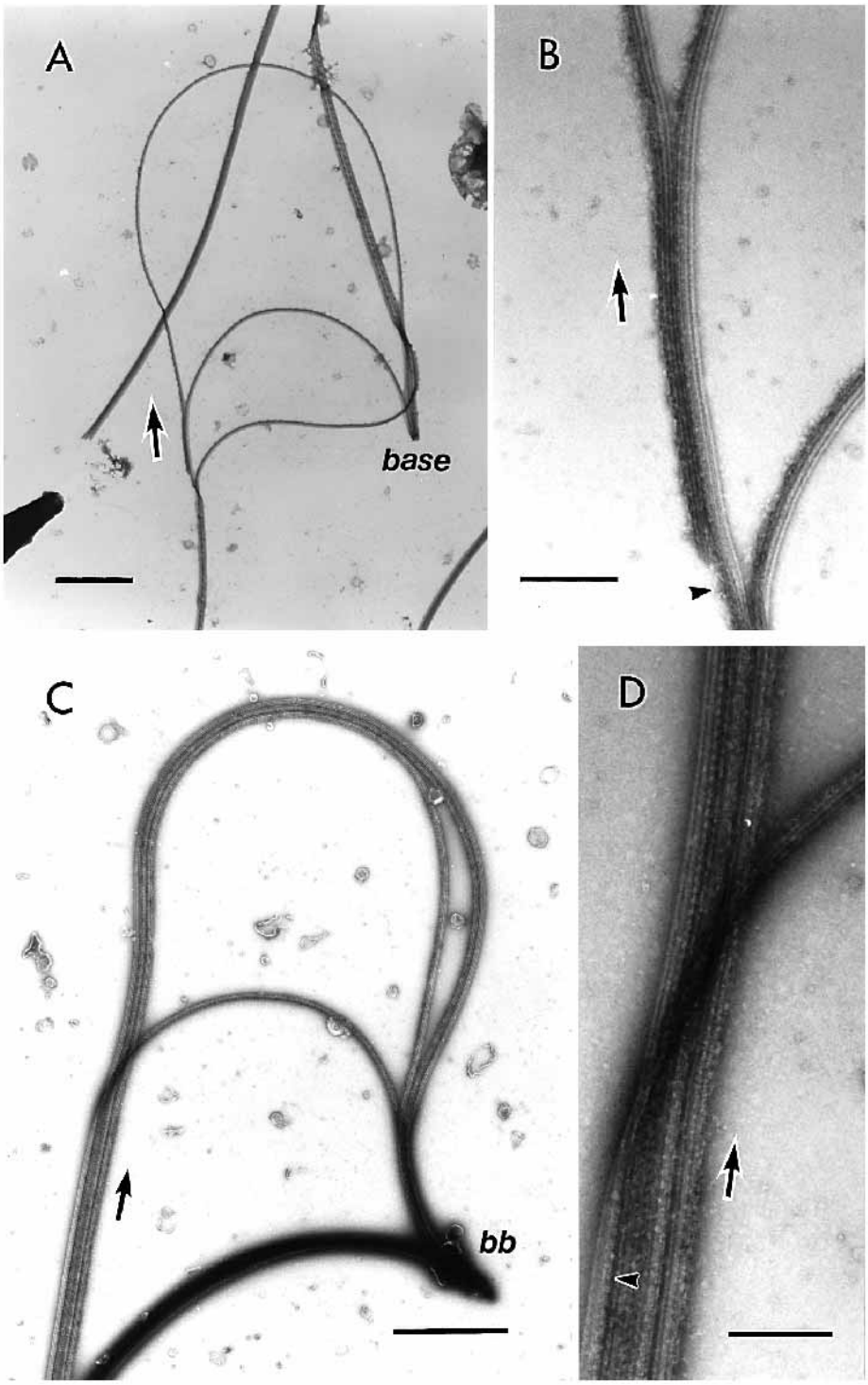

Fig. 5. Electron micrographs of sliding between doublets of sperm axonemes demembranated with Triton and millimolar calcium and treated with $MgATP^{2-}$ and elastase. (B and D) High magnification views of the vicinity of the arrows in A and C. The basal body (*bb* in C) is a marker of the proximal end of the axoneme. The dynein arms (arrowheads) generate a driving force from tip to base and cause the doublet to slide proximally (arrows). Bars: 1 μm in A and C, 0.2 μm in B and D.

axoneme formed the loops near the head or the basal body; the extruded microtubules always scattered less light in the dark-field than the axonemal bundle (Fig. 6A). The extruded microtubules often became twisted after sliding (Fig. 6B), or slid entirely off the axoneme (Fig. 6C). Sliding velocity was 14.9±4.6 μm/second (n=12) in the reactivation solution containing 0.6 mM $MgATP^{2-}$ and 0.2 mM free Ca^{2+}, which value was similar to that obtained from the reactivated sperm axonemes demembranated with Triton and millimolar calcium.

Detailed examination of the negative staining of the sliding disintegration by electron microscopy always showed that the microtubules of the larger loops slid in the proximal direction on the adjacent microtubule of the smaller loop by their own dynein arms (86 examples observed) (Fig. 7). To form this pattern, the dynein arms have generated force from base to tip.

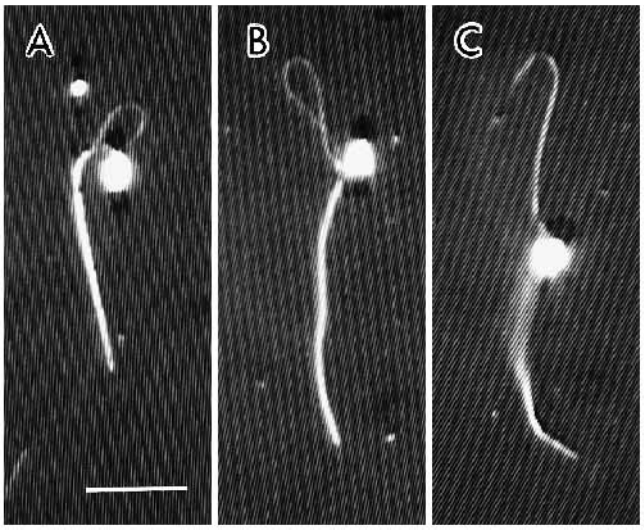

Fig. 6. Dark-field videomicrographs of sliding between doublets of quiescent sperm axonemes. Three typical patterns are shown (A-C). Doublet microtubules extruded from the axoneme formed loops near the head. The extruded microtubules were always thinner than the axonemal bundle. Bar, 15 μm.

Structure and motility of outer arm-depleted sperm axonemes

When spermatozoa were extracted in a solution containing 0.6 M KCl, the outer dynein arms were completely removed from the doublet microtubules while the inner dynein arms apparently remained intact (Fig. 8B); analysis of the cross sections of extracted sperm axonemes showed that 0.6 M KCl and 2 mM $CaCl_2$ completely removed the outer dynein arms but left 98.4% of the inner dynein arms intact (n=42 spermatozoa), while 0.15 M KCl and 2 mM $CaCl_2$ left 99.8% of the outer dynein arms and 100% of the inner dynein arms intact (n=31 spermatozoa).

These spermatozoa could be reactivated with $MgATP^{2-}$ (Fig. 9). The primary difference between the movement of the outer arm-depleted and the control spermatozoa was in beat frequency; the outer arm-depleted spermatozoa beat at approximately half the beat frequency of the control spermatozoa over a wide range of $MgATP^{2-}$ concentrations (Table 1) as reported earlier (Gibbons and Gibbons, 1973; Fox and Sale, 1987). There was no essential difference in the waveform of their bending waves, but the curvature of the bent portion of the outer arm-depleted axonemes increased somewhat, and as a consequence, the wavelength and the amplitude of the bending waves decreased (Fig. 9C). A more detailed analysis is, however, required for a better understanding of the movement of outer arm-depleted sperm axonemes (Brokaw, 1994). The direction of the circular motion of outer arm-depleted reactivated spermatozoa swimming at the upper surface of the sperm suspension depended upon the calcium concentration in a profile similar to that of intact outer arm spermatozoa (Fig. 1).

Active sliding between doublets in outer arm-depleted sperm axonemes

Exposure of spermatozoa demembranated with Triton X-100, 0.6 M KCl, and millimolar calcium to $MgATP^{2-}$ and elastase caused microtubule sliding disintegration after a certain period of beating of reactivated sperm flagella. The patterns of sliding disintegration of the outer arm-depleted axonemes are comparable to those of intact outer arm spermatozoa extracted with Triton, 0.15 M KCl, and millimolar calcium; the extruded doublet microtubules often scattered more light in dark-field illumination than the remainder. An apparent difference in the sliding disintegration between outer arm-depleted sperm axonemes and intact outer arm axonemes was sliding velocity. Sliding velocity of the doublet microtubules from outer arm-depleted sperm axonemes was 7.4±3.0 μm/second (n=13) in the reactivation solution containing 0.5 mM $MgATP^{2-}$ and 0.1 μM free Ca^{2+}, which value was approximately half that of sperm axonemes with intact outer arms.

Electron microscopic analyses of the sliding disintegration of outer arm-depleted sperm axonemes demembranated with Triton and millimolar calcium showed that the inner dynein arms generated a driving force in either direction; the inner dynein arms of the doublet microtubule of the smaller loop generated force from tip to base and made the adjacent doublet microtubules slide proximally (28 examples observed) (Fig. 10A and B), or the inner dynein arms of the doublet microtubules of the larger loop generated force from base to tip and made their doublet microtubules slide proximally (30 examples observed) (Fig. 10C and D). When spermatozoa were extracted with Triton and 0.6 M KCl in the presence of 2 mM EGTA and reactivated in the presence of high calcium concentration, most spermatozoa became quiescent with their flagella bent into a highly asymmetric cane-like form as reported earlier (Fox and Sale, 1987). When these quiescent reactivated spermatozoa were exposed to elastase, doublet microtubules slid out from the axonemes and formed loops near the head or the basal body. The extruded doublet microtubules always scattered less light under dark-field illumination than the remainder, as was seen in the intact outer arm axonemes. The sliding velocity of the doublet microtubules from outer arm-depleted sperm axonemes was 7.8±3.5 μm/second (n=16) in the reactivation solution containing 0.6 mM $MgATP^{2-}$ and 0.2 mM free Ca^{2+}, a velocity which was similar to that obtained from the outer arm-depleted sperm axonemes extracted with Triton, 0.6 M KCl, and millimolar calcium and approximately half that of quiescent sperm axonemes with intact outer arms.

Electron microscopic examinations of the microtubule sliding of quiescent reactivated sperm axonemes revealed that the doublet microtubules extruded from the outer arm-depleted axonemes and formed larger loops near the head or the basal body. They had evidently slid in the proximal direction relative to the microtubules of smaller loops by their own inner dynein arms (38 examples observed) (data not shown). This is the same direction of microtubule sliding of intact outer arm axonemes; the inner dynein arms have generated force from base to tip.

DISCUSSION

There are three important findings in the present study: (1) the direction of the power stroke of dynein arms was either base to tip or tip to base when the spermatozoa were demembranated with Triton and millimolar calcium and then disintegrated with $MgATP^{2-}$ and elastase; (2) the direction of the power stroke of dynein arms was only base to tip when the spermatozoa were demembranated with Triton in the absence of calcium and then disintegrated with $MgATP^{2-}$ and elastase;

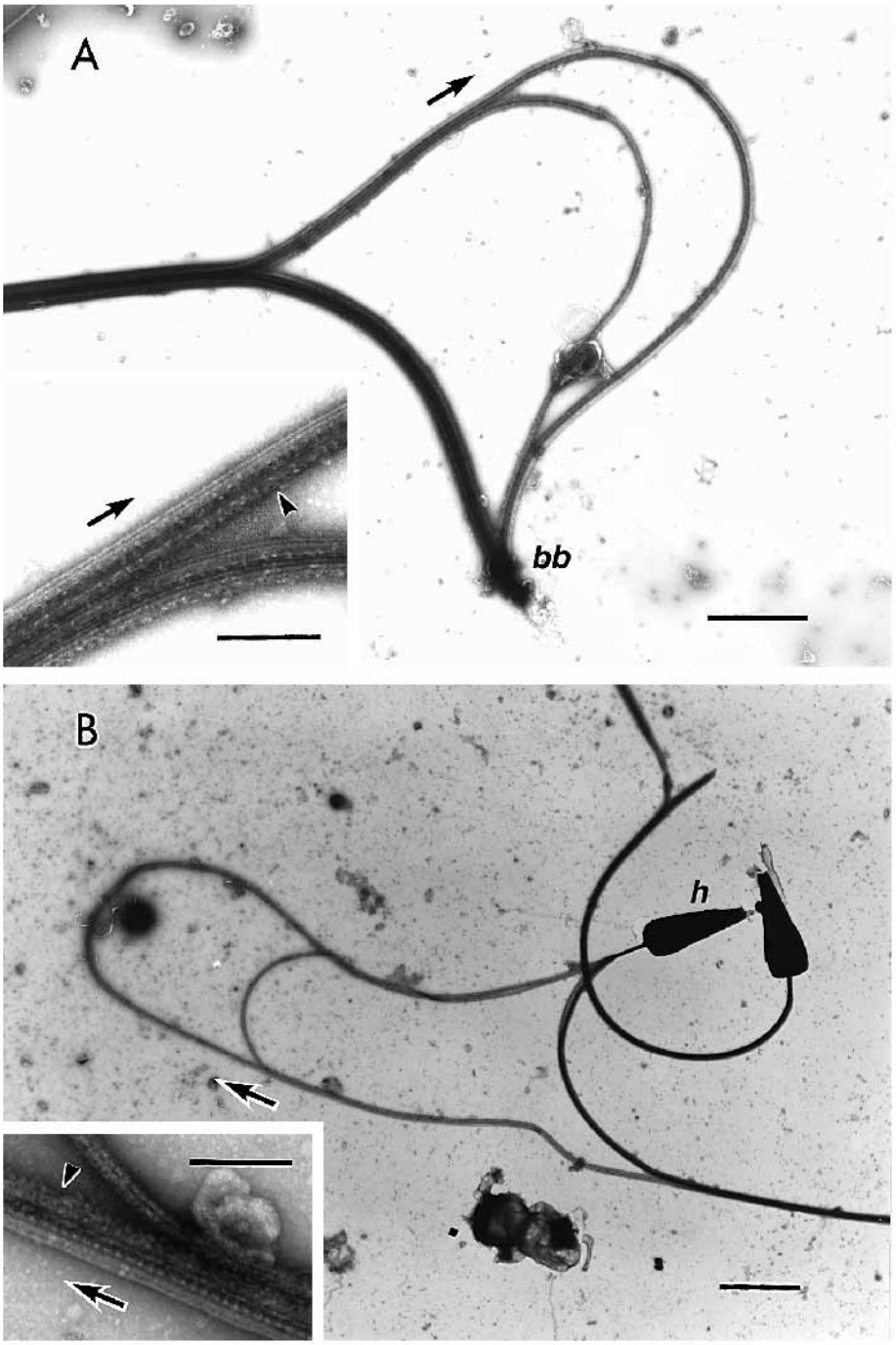

Fig. 7. Electron micrographs of sliding between doublets of quiescent sperm axonemes. The basal body (*bb* in A) or the head (*h* in B) is a marker of the proximal end of the axonemes. The insets, which are high magnification views of the vicinity of the arrows, show that the dynein arms (arrowheads) generate a driving force from base to tip and cause the doublet to slide proximally (arrows). Bars: 1 μm in A, 2 μm in B, 0.2 μm in insets.

(3) the change in the direction of the power stroke under different conditions during permeabilization was also observed in the spermatozoa from which the outer dynein arms were selectively extracted. The results obtained by most previous workers (Sale and Satir, 1977; Mogami and Takahashi, 1983; Fox and Sale, 1987; Woolley and Brammall, 1987) that dynein arms generate force only from base to tip agree exactly with our second findings. The results obtained in the present study were not artifacts arising from electron microscopy because the findings that the dynein arms of doublet microtubules of the axonemes demembranated with Triton and millimolar calcium generated force in an alternative direction corresponded closely with the discovery of the exceptional pattern of microtubule sliding disintegration, in which the extruded microtubules scattered more light under dark-field illumination than the residual doublet microtubules. This pattern had never been seen before (Sale, 1986; Fox and Sale, 1987). The function of Ca^{2+} during demembranation by Triton is unclear, but Brokaw and Nagayama (1985) suggested that axonemal calmodulin is removed by detergent extraction in the presence of millimolar calcium. Therefore, calmodulin is probably involved in regulating the direction of the power stroke of the dynein arms.

Most in vitro motility assays involving observation of microtubule gliding over a glass surface coated with dyneins and of movement of beads coated with dyneins along microtubules have shown that both axonemal and cytoplasmic

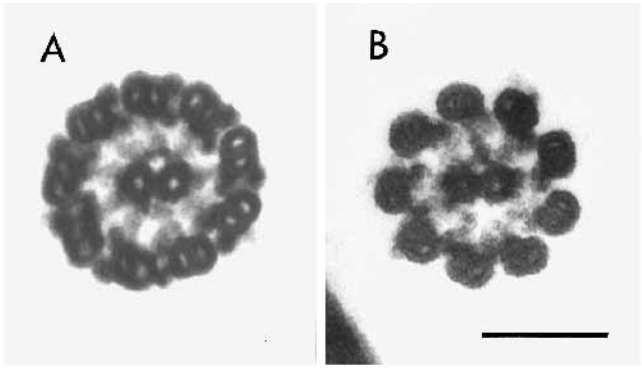

Fig. 8. Electron micrographs of a cross section of sperm axonemes extracted in the presence of 0.15 M KCl (A) and 0.6 M KCl (B). The outer dynein arms were completely extracted in the 0.6 M KCl solution (B). Bar, 0.1 μm.

dyneins produce gliding in only one direction (Paschal and Vallee, 1987; Gibbons, 1988; Vale and Toyoshima, 1988; Schnapp and Reese, 1989; Schroer et al., 1989). Nevertheless, tracks of dyneins aligned with the same polarity induce microtubule sliding in both directions in the presence of Nonidet P-40 (Mimori and Miki-Noumura, 1994), and cytoplasmic dyneins extracted from the giant amoeba, *Reticulomyxa*, cause bidirectional movements of beads along microtubules (Euteneuer et al., 1988). Furthermore, a given gyre of the helical ribbons of doublet microtubules obtained by splitting the axoneme can both lengthen and shorten due to ATP released from caged ATP (Vernon and Woolley, 1994). Taking these results and the present finding together, it is therefore likely that there is an alternative polarity of force generation by the dynein arms in intact sperm flagella.

One might have expected that the images obtained by electron microscopy could result from passive sliding of doublet microtubules because the doublet microtubules were anchored at the basal body. Nevertheless, this is highly improbable for the following reasons. We have never seen that dynein arms push the adjacent B-tubule toward the base of the axonemes when the spermatozoa are demembranated with Triton X-100 in the absence of Ca^{2+} and disintegrated with ATP and elastase, and hence the appearance of dynein arms pushing the adjacent B-tubule toward the base is very likely caused by the high Ca^{2+} concentration at the time of permeabilization. Dark-field light microscopic examination of ATP-induced sliding disintegration of the axoneme showed that the doublet microtubules forming different loops disintegrated independently; the doublet microtubules of the larger loops continued sliding, even though they were in contact with only the doublet microtubules of the smaller loops because their distal ends had left the residual doublet microtubules (Fig. 3). This was clearly demonstrated by electron microscopy; no doublet microtubule inducing passive sliding of the largest loop exists (Fig. 5A). Because doublet microtubules were fixed under conditions in which the dynein arms were expected to be active, the loops formed by passive sliding would immediately disappear if the dynein arms could stroke from base to tip.

In the present study, elastase was used instead of trypsin because trypsin may remove calcium sensitivity from the axoneme (Mogami and Takahashi, 1983), and most calmodulin-binding proteins are extremely sensitive to trypsin treatment (Tash, 1990). The bidirectional power stroke of the dynein arms seen in the present study therefore seems to result from both the calcium environment at the time of permeabilization and from digestion by elastase. However, trypsin was not used in the procedures of in vitro motility assays mentioned above, in which all dyneins move unidirectionally on microtubules toward their minus ends; the calcium environment at the time of permeabilization may be essential for maintaining the regulation that originally existed in the sperm flagella.

The spermatozoa having yaw counterclockwise at the upper surface of the sperm suspension disintegrated by active sliding of doublet microtubules and showed the characteristic pattern,

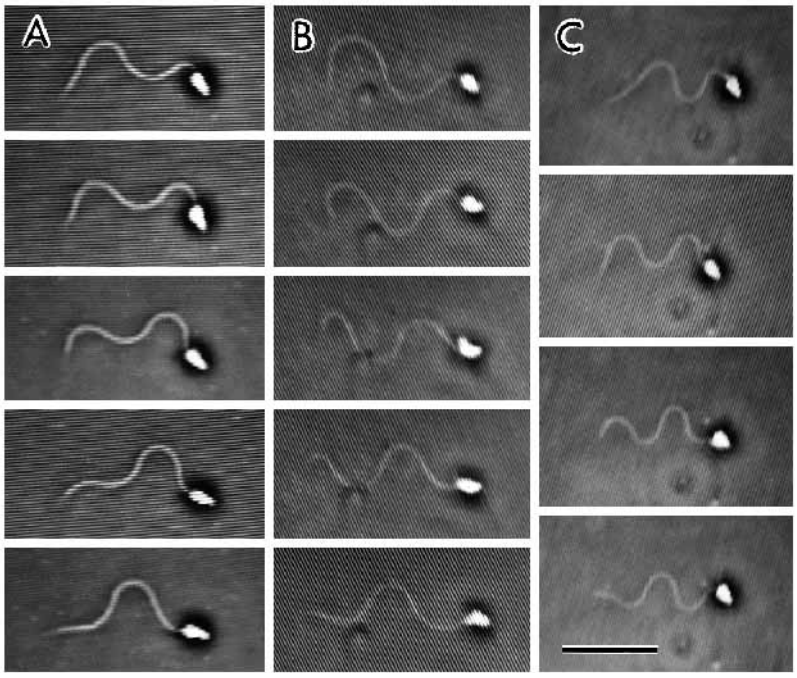

Fig. 9. Phase-contrast videomicrographs of flagellar movements of intact (A) and reactivated spermatozoa (B and C). The spermatozoa were demembranated with Triton X-100 and millimolar calcium in the presence of 0.15 M KCl (B) or 0.6 M KCl (C) and then reactivated with 0.5 mM $MgATP^{2-}$ and 0.1 μM free Ca^{2+}. The spermatozoa swimming close to the coverslip surface were recorded at 200 images per second. The time interval between successive images was 5 milliseconds (A and B) and 10 milliseconds (C). Beat frequency was 33 Hz (A), 34 Hz (B), and 18 Hz (C) at 19°C. Bar, 20 μm.

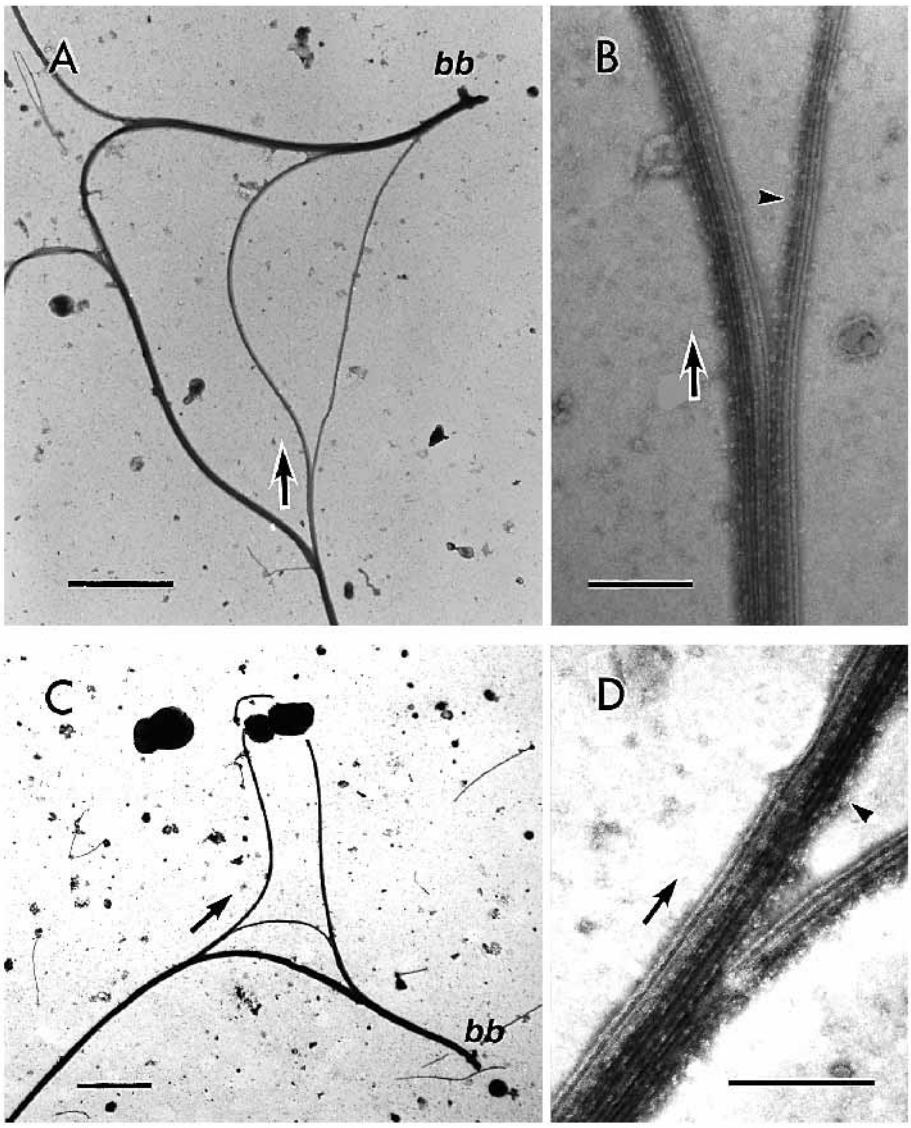

Fig. 10. Electron micrographs of sliding between doublets of outer arm-depleted sperm axonemes. The spermatozoa were demembranated with Triton, 0.6 M KCl, and millimolar calcium and disintegrated with $MgATP^{2-}$ and elastase. The basal body (*bb* in A and C) is a marker of the proximal end of the axonemes. (B and D) High magnification views of the vicinity of the arrows in A and C. The inner dynein arms (arrowheads) generate a driving force not only from tip to base (A and B) but also from base to tip (C and D) and cause the doublet to slide proximally (arrows). Bars: 2 μm in A and C, 0.2 μm in B and D.

in which the extruded doublet microtubules were thicker than the residual doublet microtubules. If it is accepted that this pattern of sliding disintegration is caused by the baseward power stroke of dynein arms as mentioned above, then the direction of the power stroke of dynein arms may determine the direction of the yawing motion of the reactivated spermatozoa. Because a one-to-one correspondence between the direction of the yawing motion of the spermatozoa near an interface and that of the rolling motion of the spermatozoa around their long axis is quantitatively proved (Ishijima and Hamaguchi, 1992), the direction of the power stroke of dynein arms may regulate the sense of the three-dimensional geometry of beating sperm flagella. The result of no significant difference in the calcium-dependency of chirality between the reactivated sperm axonemes having only inner arms and those having both inner and outer arms suggests that the three-dimensional shape of beating sperm flagella is regulated mainly by the inner dynein arms.

We thank Dr B. A. Afzelius for critical reading of the manuscript and several suggestions and Dr T. Nakazawa for his kind hospitality. We also thank the director, Dr S. Nemoto, and the staff of the Tateyama Marine Laboratory of the Ochanomizu University for providing materials.

REFERENCES

Bers, D. M., Patton, C. W. and Nuccitelli, R. (1994). A practical guide to the preparation of Ca^{2+} buffers. *Meth. Cell Biol.* **40**, 3-29.

Brokaw, C. J. (1980). Elastase digestion of demembranated sperm flagella. *Science* **207**, 1365-1367.

Brokaw, C. J. and Nagayama, S. M. (1985). Modulation of the asymmetry of sea urchin sperm flagellar bending by calmodulin. *J. Cell Biol.* **100**, 1875-1883.

Brokaw, C. J. (1986). Sperm motility. *Meth. Cell Biol.* **27**, 41-56.

Brokaw, C. J. (1991). Calcium sensors in sea urchin sperm flagella. *Cell Motil. Cytoskel.* **18**, 123-130.

Brokaw, C. J. (1994). Control of flagellar bending: A new agenda based on dynein diversity. *Cell Motil. Cytoskel.* **28**, 199-204.

Euteneuer, U. and McIntosh, J. R. (1981). Polarity of some motility-related microtubules. *Proc. Nat. Acad. Sci. USA* **78**, 372-376.

Euteneuer, U., Koonce, M. P., Pfister, K. K. and Schliwa, M. (1988). An ATPase with properties expected for the organelle motor of the giant amoeba, *Reticulomyxa*. *Nature* **332**, 176-178.

Fox, L. A. and Sale, W. S. (1987). Direction of force generated by the inner row of dynein arms on flagellar microtubules. *J. Cell Biol*. **105**, 1781-1787.

Gibbons, B. H. and Gibbons, I. R. (1973). The effect of partial extraction of dynein arms of the movement of reactivated sea urchin sperm. *J. Cell Sci*. **13**, 337-357.

Gibbons, B. H. and Gibbons, I. R. (1980). Calcium-induced quiescence in reactivated sea urchin sperm. *J. Cell Biol*. **84**, 13-27.

Gibbons, I. R. (1981). Cilia and flagella of eukaryotes. *J. Cell Biol*. **91**, 107s-124s.

Gibbons, I. R. (1988). Dynein ATPases as microtubule motors. *J. Biol. Chem*. **263**, 15837-15840.

Goldstein, D. A. (1979). Calculation of the concentration of free cations and cation-ligand complexes in solutions containing multiple divalent cations and ligands. *Biophys. J*. **26**, 235-242.

Ishijima, S. and Hamaguchi, Y. (1992). Relationship between direction of rolling and yawing of golden hamster and sea urchin spermatozoa. *Cell Struct. Funct*. **17**, 319-323.

Ishijima, S., Hamaguchi, M. S., Naruse, M., Ishijima, S. A. and Hamaguchi, Y. (1992). Rotational movement of a spermatozoon around its long axis. *J. Exp. Biol*. **163**, 15-31.

Ishijima, S. and Hamaguchi, Y. (1993). Calcium ion regulation of chirality of beating flagellum of reactivated sea urchin spermatozoa. *Biophys. J*. **65**, 1445-1448.

Ishijima, S. (1995). High-speed video microscopy of flagella and cilia. *Meth. Cell Biol*. **47**, 239-243.

Mimori, Y. and Miki-Noumura, T. (1994). ATP-induced sliding of microtubules on tracks of 22S dynein molecules aligned with the same polarity. *Cell Motil. Cytoskel.* **27**, 180-191.

Mogami, Y. and Takahashi, K. (1983). Calcium and microtubule sliding in ciliary axonemes isolated from *Paramecium caudatum*. *J. Cell Sci*. **61**, 107-121.

Mori, M. and Miki-Noumura, T. (1992). Inhibition of gliding movement by calcium in doublet microtubules on *Tetrahymena* ciliary dyneins *in vitro*. *Exp. Cell Res*. **203**, 483-487.

Paschal, B. M. and Vallee, R. B. (1987). Retrograde transport by the microtubule-associated protein MAP 1C. *Nature* **330**, 181-183.

Sale, W. S. (1986). The axonemal axis and Ca^{2+}-induced asymmetry of active microtubule sliding in sea urchin sperm tail. *J. Cell Biol*. **102**, 2042-2052.

Sale, W. S. and Satir, P. (1977). Direction of active sliding of microtubules in *Tetrahymena* cilia. *Proc. Nat. Acad. Sci. USA* **74**, 2045-2049.

Schnapp, B. J. and Reese, T. S. (1989). Dynein is the motor for retrograde axonal transport of organelles. *Proc. Nat. Acad. Sci. USA* **86**, 1548-1552.

Schroer, T. A., Steuer, E. R. and Sheetz, M. P. (1989). Cytoplasmic dynein is a minus end-directed motor for membranous organelles. *Cell* **56**, 937-946.

Sloboda, R. D. (1992). Methods for the purification and assay of microtubule-associated motility proteins. In *The Cytoskeleton* (ed. K. L. Carraway and C. A. C. Carraway), pp. 167-196. IRL Press, Oxford.

Tamm, S. L. (1989). Control of reactivation and microtubule sliding by calcium, strontium, and barium in detergent-extracted macrocilia of *Beroë*. *Cell Motil. Cytoskel.* **12**, 104-112.

Tash, J. S. (1990). Role of cAMP, calcium, and protein phosphorylation in sperm motility. In *Controls of Sperm Motility: Biological and Clinical Aspects* (ed. C. Gagnon), pp. 229-240. CRC Press, Boca Raton.

Vale, R. D. and Toyoshima, Y. Y. (1988). Rotation and translocation of microtubules in vitro induced by dyneins from Tetrahymena cilia. *Cell* **52**, 459-469.

Vernon, G. G. and Woolley, D. M. (1994). Direct evidence for tension development between flagellar doublet microtubules. *Exp. Cell Res*. **215**, 390-394.

Walter, M. F. and Satir, P. (1979). Calcium does not inhibit active sliding of microtubules from mussel gill cilia. *Nature* **278**, 69-70.

Woolley, D. M. and Brammall, A. (1987). Direction of sliding and relative sliding velocities within trypsinized sperm axonemes of *Gallus domesticus*. *J. Cell Sci*. **88**, 361-371.

(Received 27 February 1996 – Accepted 4 September 1996)